Hindawi
Advances in Materials Science and Engineering
Volume 2019, Article ID 7657234, 10 pages
https://doi.org/10.1155/2019/7657234

Research Article

Fracture of Parallel Strand Bamboo Composite under Mode I Loading: DCB Test Investigation

Yurong Shen,[1,2] Dongsheng Huang,[1] Ying Hei Chui,[2] and Chunping Dai[3]

[1]*National Engineering Research Center of Biomaterials, Nanjing Forestry University, Nanjing 210037, China*
[2]*Department of Civil and Environment Engineering, University of Alberta, Edmonton T6G 1H9, Canada*
[3]*Department of Wood Science, The University of British Columbia, Vancouver, Canada V6T 1Z4*

Correspondence should be addressed to Dongsheng Huang; dshuang@njfu.edu.cn

Received 10 July 2019; Revised 30 August 2019; Accepted 6 September 2019; Published 23 September 2019

Guest Editor: Grzegorz Lesiuk

This paper describes the experimental studies on Mode I fracture of parallel strand bamboo (PSB) by the double cantilever beam (DCB) test. R-curves based on the elementary beam theory and specimen compliance are proposed in order to overcome the difficulties to monitor the crack propagation during experiments. The results demonstrate that the energy release rate (ERR) is influenced by the specimen geometry, i.e., the specimen width and initial crack length. The ERR at the plateau level is similar for the range of the analyzed widths ($B = 20$, 40, and 60 mm), while it decreases with width increasing up to 80 mm and 100 mm. The energy release rate for PSB specimens would verge to a stable value with the width increasing up to a specific value, while the value of the energy release rate will be influenced by the initial crack length. Consequently, the DCB tests also show that the obtained R-curve in this study is not a material property.

1. Introduction

Parallel strand bamboo (PSB) is manufactured by parallelly gluing bamboo strands together under controlled temperature and pressure. Because bamboo strips are parallelly glued along the longitudinal direction and uniformly distributed over the transverse direction, PSB can be considered as a unidirectional and orthotropic fibrous composite, as shown in Figure 1 [1]. More recently, PSB wins growing interests as an alternative of wood composites for construction engineering in China due to its fast-growing feature and excellent structural performance. Aimed at the structural use, the failure modes of combined compression and bending PSB members were studied by Huang et al. [2–4]. It was found that the fracture along the fiber interfaces was one of the major failure modes of PSB composites. Once a PSB member subjected to an increasing external load, the initial deflects, such as microvoids and microcracks, could be advancing or growing into macrocracks and consequently result in catastrophic failure of structures. Therefore, the fracture of PSB composite is one of the major concerns in PSB structural design.

The objective of the present study is to investigate the Mode I fracture properties and to measure the fracture toughness of the PSB composite through DCB experiments, which is one of the necessities for establishing design allowable values used in damage tolerance analysis of PSB structures.

The double cantilever beam (DCB) test [5–7], a standard test procedure prescribed in ASTM D5528-13 [8], was employed as the test procedure in this study. The test uses a rectangular specimen with different widths, different initial crack lengths, and constant thickness. It contains a preimplanted, nonadhesive insert or crack as an initial delamination. The opening load is applied perpendicular to the initial crack surface to induce the Mode I crack. Such a test analysis is based on the beam theory, and the fracture toughness can be measured through the energy release rate (ERR) for orthotropic fibrous composites. The ERR can be obtained by various methods, including direct area integration of loading-unloading curves or by means of

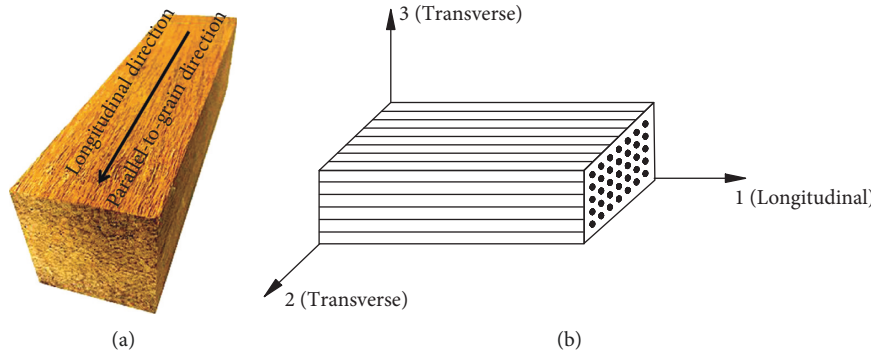

Figure 1: (a) Photograph of PSB. (b) Principal directions of PSB.

compliance measurements [9]. Since the data reduction of DCB test is easier than the other test approaches [10, 11], it is now the most popular method used to determine Mode I fracture toughness.

Recommended by ASTM and ISO standards [9, 12, 13], the energy release rate can be estimated through the change of compliance. Theoretically, it can be obtained by differentiating the specimen compliance, C, with respect to the crack length a, i.e., $G = (P^2/2B)(\partial C/\partial a)$ [14–18], where P is the applied load and B the width of the specimen. In the frame of linear fracture mechanics, the root condition is supposed to be fully built-in; hence, the compliance equation can be given by simple beam theory, i.e., $C = 8a^3/BEh^3$ [9]. Nevertheless, because of the fuzzy boundary conditions at the end of opening arms, the compliance equation $C(a)$ cannot be determined without controversy. On the other hand, the crack length cannot be measured either with desired precision. Therefore, various data reduction methods were developed to overcome this disadvantage, such as the area method, in which the compliance equation was built through data fitting for tests [19, 20]. Hashemi et al. [21] compared the different data reduction methods for obtaining the energy release rate of fibrous composites. They proposed that the correction of crack length was necessary in the beam theory-based method because the end of opening arms was not perfectly clamped. They developed the corrected beam theory (CBT), providing a correction in the crack length based on a compliance calibration. However, the fracture mechanism of fibrous composite is much complicated than that of brittle materials. The major aspect is that the microvoids coalescing, fine cracks extending, and fiber bridging lead to a large fracture process zone (FPZ) in front of the crack tip, which makes the clear location of the crack tip impracticable [22–25]. Furthermore, the development of the large FPZ in the crack-tip front delays the fracture of specimen, which consequently makes the built-in assumption no longer valid. It has been well recognized that the use of elementary beam theory with the built-in assumption at the crack tip has a significant error for calculating the energy release rate of fibrous composites [26]. To date, there is no method available to exactly identify the crack tip for the DCB test of fibrous composites. For this reason, extensive researches have been carried out to avoid locating the crack tip [27–32]. Among these researches, the concept of equivalent linear elastic fracture mechanics (LEFM) was widely accepted to deal with the fracture with a large FPZ [31]. According to the concept of equivalent LEFM, the increasing of compliance, owing to the development of FPZ or main crack propagation with FPZ, is attributed to the elastic crack which equals to the actual crack with its FPZ [33]. Therefore, the crack length can be estimated according to the associated compliance obtained by experiments. Furthermore, the R-curve can also be measured using only a monotonic load-displacement record.

In the present study, the data reduction method was based on the theory of equivalent LEFM. Compliance calibration was introduced to determine the crack length. The direct integral approach was adopted to calculate the energy release rate.

2. Data Reduction Scheme

Figure 2 illustrates the principle of evaluating energy release rate based on the theory of equivalent LEFM. In the schematic load-displacement curve (F, δ), two consecutive points $M_1(\delta(a_1), F(a_1))$ and $M_2(\delta(a_2), F(a_2))$ corresponding to two different crack lengths a_1 and a_2, respectively, are selected. Suppose that the crack extends from length a_1 to a_2 with a small amount of propagation increment Δa and that the load-displacement trajectory goes from M_1 to M_2; thus, the shadow area circulated by the dashed lines OM_1, and OM_2 and the segment of load-displacement M_1M_2 must be equal to the energy released as the crack growth of the extension Δa [19]. Therefore, the energy release rate can be calculated by

$$G_R = \frac{1}{b\Delta a}\left[\frac{1}{2}P(a_1)\delta(a_2) - \frac{1}{2}P(a_2)\delta(a_1)\right], \quad (1)$$

where P and δ stand for the applied load and associated displacement at loading position, respectively. The crack length $a_i\,(i = 1, 2)$ can be determined from the test compliance $C(a_i) = (\delta(a_i))/(P(a_i))$. According to the beam theory, the compliance can be calculated by [34]

$$C(a) = \frac{a^3}{E_L I} + \frac{6a}{5G_{LT}A}, \quad (2)$$

where E_L is the longitudinal elastic modulus, G_{LT} is the shear modulus in LT plane, i.e., the 12 or 13 plane as shown in Figure 1(b), I is the inertia moment of the cross section, and

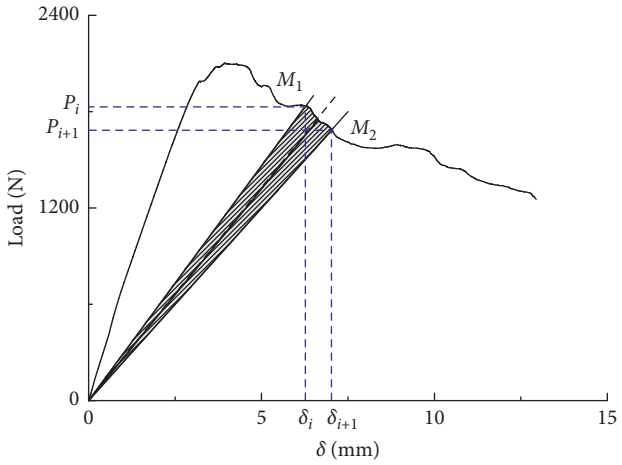

Figure 2: Schematic diagram of the evaluation of the resistance to crack growth (G_R).

A is the area of cross section. Once the compliance $C(a_i)$is obtained by experiment and the crack length can be determined by resolving equation (2) or by numerical iteration in terms of the following equation:

$$a_i = \left[\frac{3E_L I\lambda C(a_i)}{2\left(1+\left(3E_L h^2/10G_{LT}a_{i-1}^2\right)\right)}\right]^{(1/3)}, \quad (3)$$

where $\lambda = \overline{C}_0/C_0$ is the calibration parameter to eliminate the system error of the experiment, in which C_0 is the test compliance corresponding to the initial crack length a_0 and $\overline{C}_0$ stands for the theoretical compliance corresponding to the initial crack length calculated by equation (2).

3. Experimental Investigation

3.1. Materials. The test PSB was provided by Feiyu Bamboo Products, Jianghxi, China. The material density was 1.26 g/cm^3, and the moisture content was 11%. Mechanical properties in parallel-to-grain direction, which are involved in test analysis, were pretested following the method recommended in ASTM D143-14 [35], and the results are collected in Table 1, where the subscripts L and T are the parallel-to-grain direction and perpendicular-to-grain direction, respectively, and v represents Poisson's ratio of PSB.

3.2. Specimen Preparation. The geometry of DCB specimen is shown in Figure 3. The dimensions of DCB specimen were determined referring to the standard test procedure addressed in ASTM D5528-13 [8]. In this method, the DCB dimension was designed to ensure the damage zone or nonlinear deformation developed along the delamination front and the stable crack growth can be achieved.

Totally four groups of specimens with different initial crack lengths and different widths were prepared, as illustrated in Table 2, in which each group consists of the same initial crack length and 5 types of specimens with different widths. A label system was designed to identify the specimen. In this system, the latter *A*, *B*, *C*, and *D* correspond to the initial crack length of 34 mm, 67 mm, 100 mm, and 134 mm, respectively. The number prior to the letter of the group name stands for the width of the specimen, as shown in Table 2. The initial crack was firstly introduced by a 1.5 mm thick saw kerf; afterwards, precrack with length about 1 mm was extended by using a cutting blade [10]. At the end of the DCB test, two bolt holes of 8 mm in diameter were drilled for the sake of joining DCB specimen to the actuator of the test machine, as illustrated in Figure 3.

Table 1: Mechanical properties of PSB composites in parallel-to-grain direction.

Items	E_L (MPa)	G_{LT} (MPa)	v_{LT}	v_{TL}
Mean	15363	4890	0.32	0.05
CV (%)	9.575	12.31	12.3	25.6

3.3. Test Procedure. The fracture tests were performed on a servo-hydraulic universal test machine of 20 kN capacity in room ambient circumstance. The test setup is illustrated in Figure 4(a). The specimen was joined to the load actuator through two steel rods of 7.5 mm diameter, as shown in Figure 4(b). Loading was controlled by the displacement of a moveable actuator at the speed of 1.0 mm/min. A microscope digital camera was mounted in front of the specimen to monitor the crack propagation and take the images of the crack tip. The applied load and the displacement at loading position were simultaneously recorded at a frequency of 10 Hz. The opening displacement at the initial crack tip was measured by using a clip-on gauge (COD gauge) symmetrically fixed at the two sides of the crack tip through embedded aluminum flakes (Figure 4(b)). The crack length during propagation can be observed by using the microscopic camera, as shown in Figure 4(b).

4. Test Results

4.1. Load-Displacement Curve. Figure 5 illustrates a typical load-displacement curve. Roughly three stages can be observed. The first one (stage I) is no-damage stage from origin to the proportional limit point where the curve deviates from its original direction. The load-displacement curve exhibits perfect linearity in this stage. Once the load exceeds the point of proportional limit (stage II), damage onset extends and coalesces to form the fracture process zone (FPZ) and consequently leads to the compliance augment and the curve continuously deviates from its original direction as the load increases. Hence, this stage can be understood as the stage of FPZ development. When the FPZ fully developed, the load-displacement curve would reach its critical point, where the load reached its maximum value and the crack propagation began. Hence, the third stage (stage III) is the crack propagation stage.

Figure 6 presents the load-displacement profiles of the specimens. For the specimens of Group A, the load-displacement curve sharply declines once the load reaches the maximum value, which indicates that the crack

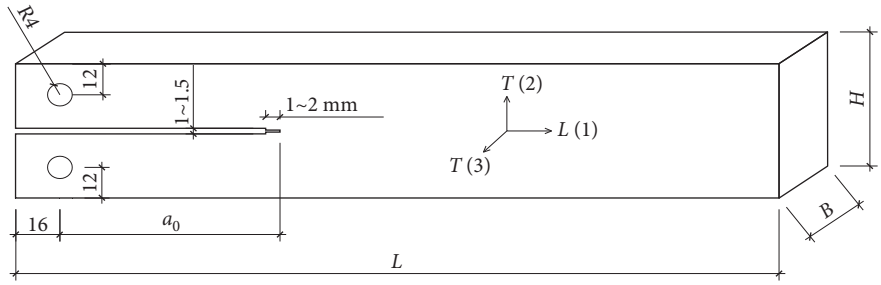

Figure 3: The configurations of DCB specimens.

Table 2: Dimensions of DCB specimens.

Group	Label	a_0 (mm)	L (mm)	B (mm)	H (mm)	a_0 (L)	Number
	20-A			20			
	40-A			40			
A	60-A	34	350	60	50	0.097	3
	80-A			80			
	100-A			100			
	20-B			20			
	40-B			40			
B	60-B	67	350	60	50	0.191	3
	80-B			80			
	100-B			100			
	20-C			20			
	40-C			40			
C	60-C	100	350	60	50	0.286	3
	80-C			80			
	100-C			100			
	20-D			20			
	40-D			40			
D	60-D	134	350	60	50	0.383	3
	80-D			80			
	100-D			100			

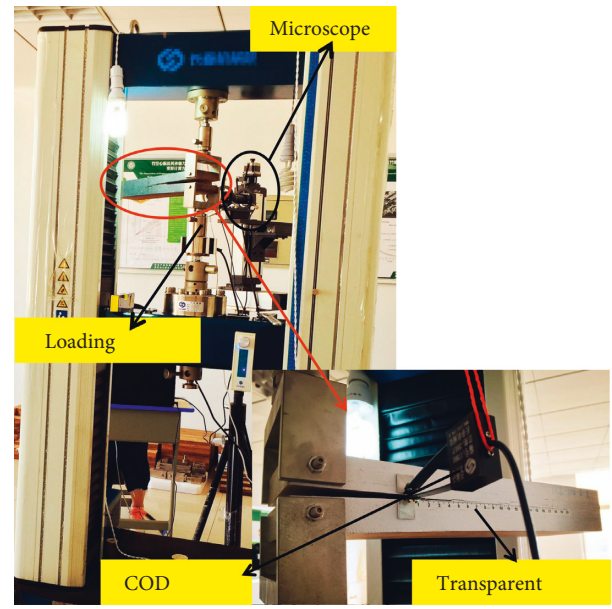

(a)

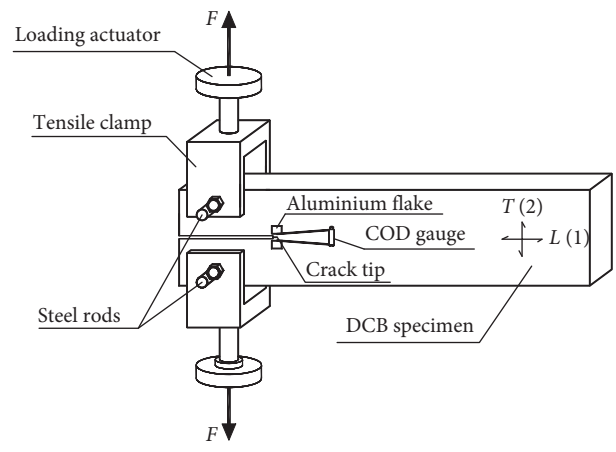

(b)

Figure 4: (a) Experimental setup of the DCB test. (b) Schematic diagram of the DCB test.

propagation is unstable. For the specimens in Groups B, C, and D with longer initial crack length, the load-displacement profile slowly declines in post-summit segments. Furthermore, the load-displacement profile declined more slowly with longer initial crack length, which indicated that the stability of crack propagation is sensitive to the initial crack length. Therefore, enough initial crack length is needed for obtaining stable crack propagation. In the present study, the ratios of initial crack length to ligament length of Groups B, C, and D are 0.191, 0.286, and 0.383, respectively, and their crack propagates in a stable and ductile manner, which means specimens with the ratio of Groups B, C, and D can be used to determine the fracture properties.

The second factor is the width scaling which has a significant influence on fiber bridging in the wake of the crack, consequently affecting the delamination behavior. As shown in Figure 7, the load-displacement curves for partial specimens are presented with the same initial crack length but different widths. It can be concluded that the crack grows in a "thumbnail" shape [36] under constant or decreasing load, while the overall displacement is increased. The "thumbnail" theory means that the crack extends mainly from the center of the thickness of specimens, while the edge regions are plastically deformed. Therefore, with the width increasing, the energy release rate

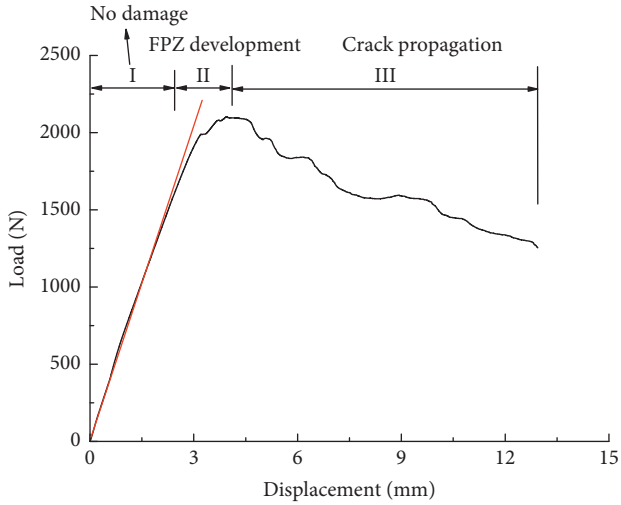

Figure 5: A typical load-displacement curve.

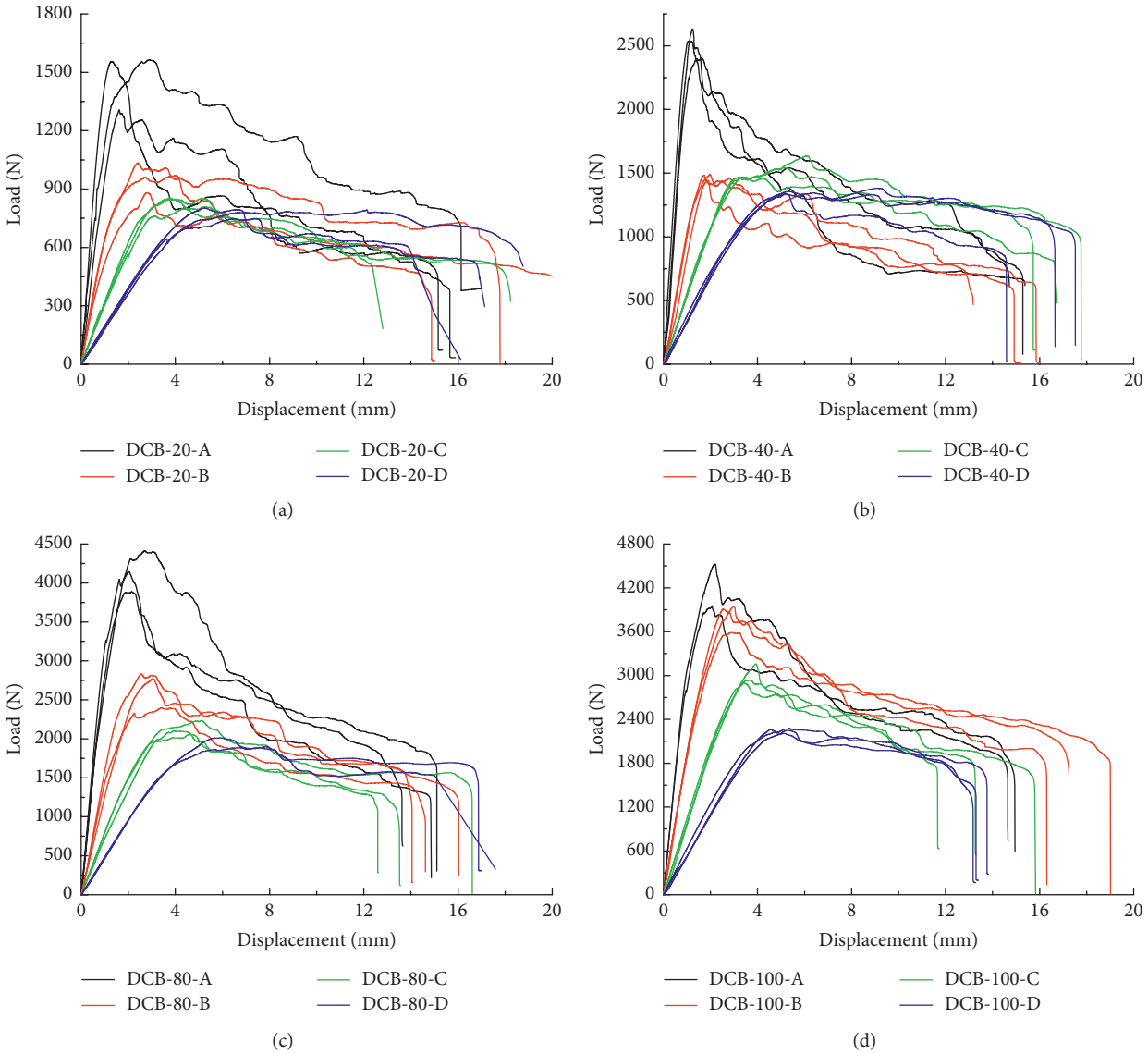

Figure 6: Load-displacement curves of all tested DCB specimens with different initial crack lengths in the same width: (a) width $B = 20$ mm; (b) width $B = 40$ mm; (c) width $B = 80$ mm; and (d) width $B = 100$ mm.

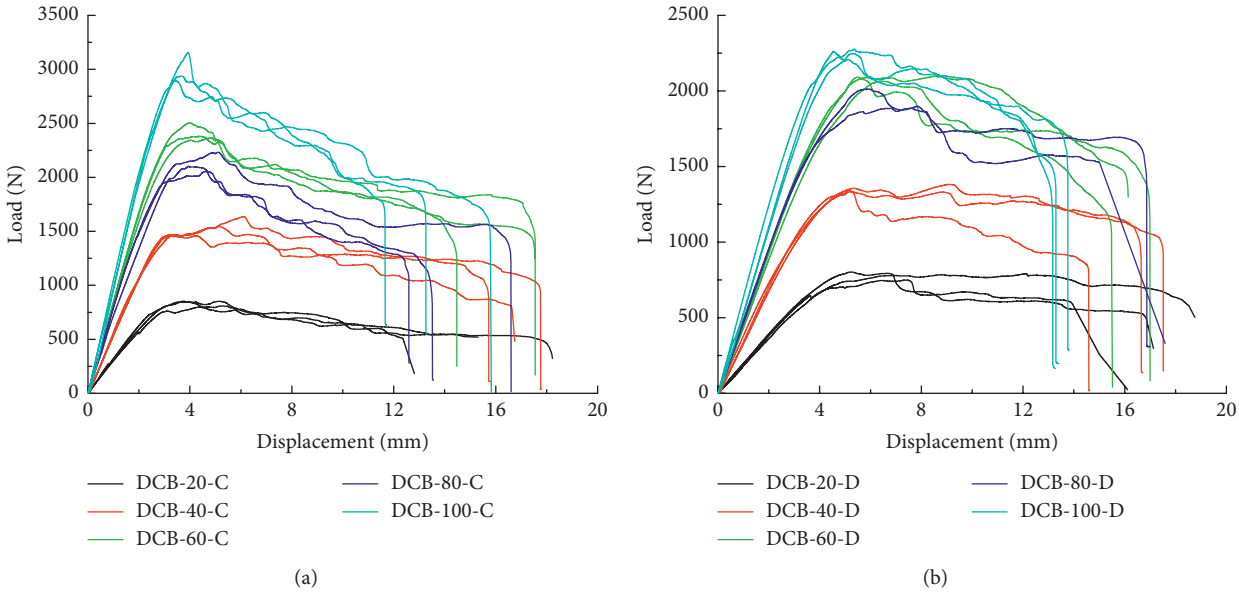

Figure 7: Load-displacement curves of DCB specimens with different widths in the same initial crack length: (a) initial crack length $a_0 = 100$ mm; (b) initial crack length $a_0 = 134$ mm.

of DCB specimens for PSB composite would converge to a stable value.

It is worth mentioning that only partial specimens exhibit their load-displacement curves or R-curves in later analysis due to the similar tendency of these curves. Moreover, because of the manufacturing defects for some PSB specimens, the data cannot be used to analyze the energy release rate in the DCB test. Therefore, some specimens present two lines in partial load-displacement curves or R-curves.

4.2. Fracture Process Zone. Damage begins when the external load exceeds its proportional limit, which is characterized by local microcracks at the crack tip front zone. This damaged zone is comprised of microcracks between the grains or through the grains. The microcracks are consequently extended and coalesced to form macrocracks and local microcracks at the advancing crack tip front as the external load increases. This fracture process and damaged zone can be called fracture process zone (FPZ). Before the load reaches its maximum value, the crack interfaces are bonded by fiber bridges which either rupture or peel off from the crack surfaces. This fracture mechanism leads to a large FPZ which can be observed at the crack tip front before crack propagation, as shown in Figure 8. Due to the restriction of fiber bridges, the strain energy is smoothly consumed through the fibrous rupture or pull-off, which leads to stable crack propagation and a rising R-curve.

Several micrographs were taken from the tested specimens at the fracture surfaces using the scanning electron microscope (SEM), as shown in Figure 9. Figure 9(a) exhibits the typical fracture surface with a limited amount of fiber pull-out in the debonding plies, which is presented with higher magnitude in Figure 9(b). The pull-out process could have created a fibre-bridged zone in the wake of the advancing crack tip. During the whole experiment, the growth and eventual stabilization of this fibre-bridged zone could account for the tendency observed in later R-curves.

4.3. R-Curve Measurement. Energy release rate for each test specimen was measured by the method addressed in Section 2. The R-curves of partial DCB specimens with different widths and different initial crack lengths corresponding to specific thickness are presented in Figures 10 and 11. It was observed that the energy release rate increases up to a steady-state toughness after the initiation of delamination. As illustrated in Section 4.2, the fiber bridging effect during the whole crack propagation led to eventual stabilization of crack growths for all tested specimens. Meanwhile, the results also implied that the R-curve obtained in this study was not a material property, i.e., it depended on specimen geometry. Consequently, when the crack starts to propagate, the bridging zone is created. By developing the bridging zone length, the strain energy release rate increases up to the steady-state fracture toughness. The length between the initial crack length and crack length corresponding to the steady-state fracture toughness is called as the steady-state bridging zone length. From Figure 10, the value of the energy release rate was always affected by the initial crack length. The major reason may be that the steady-state bridging zone of PSB specimens was always influenced by the preimbedded crack.

From Figure 11, it can also be concluded that the energy release rate of DCB specimens for the PSB composite would verge to a stable value with the width increasing up to a specific value, which will be identified in the future DCB tests for PSB specimens. As illustrated in the abovementioned "thumbnail" theory, the width scaling has

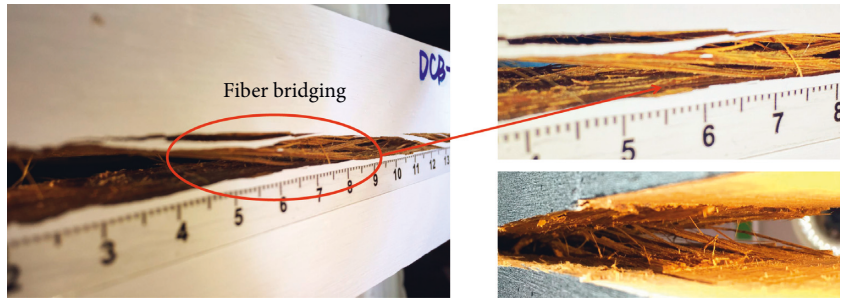

Figure 8: The fiber bridging phenomenon of DCB specimens.

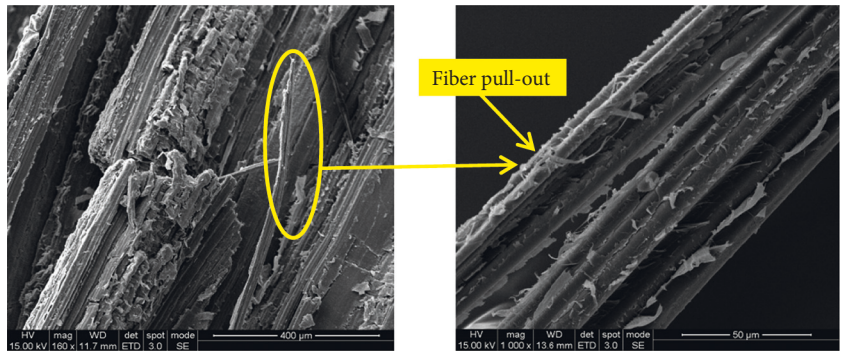

Figure 9: (a) SEM micrograph of the DCB specimens' fracture surface for PSB composite. (b) Fiber pull-out with higher magnitude.

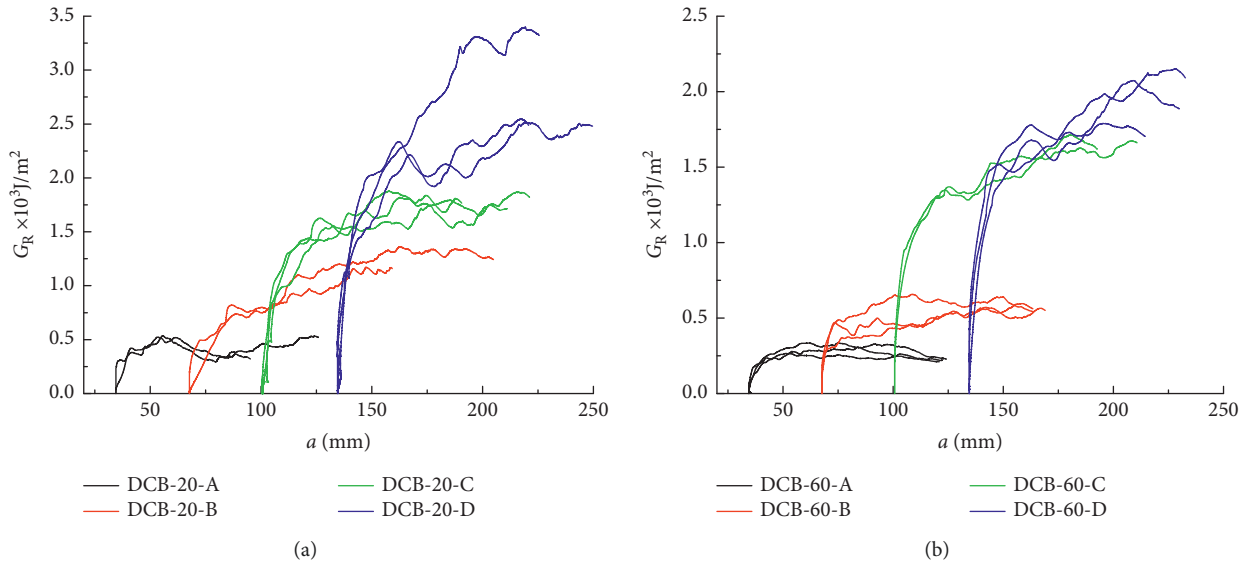

Figure 10: R-curves of DCB specimens with different initial crack lengths on the same width: (a) width $B = 20$ mm; (b) width $B = 40$ mm.

a significant effect on fiber bridging in the wake of the crack, which make the crack grow in a "thumbnail" shape, i.e., the crack extends mainly from the center of specimens, while the edge regions are plastically deformed. Therefore, the energy release rate of DCB specimens for the PSB composite would converge to a stable value with the increasing width. Table 3 gives the average fracture toughness for partial test samples.

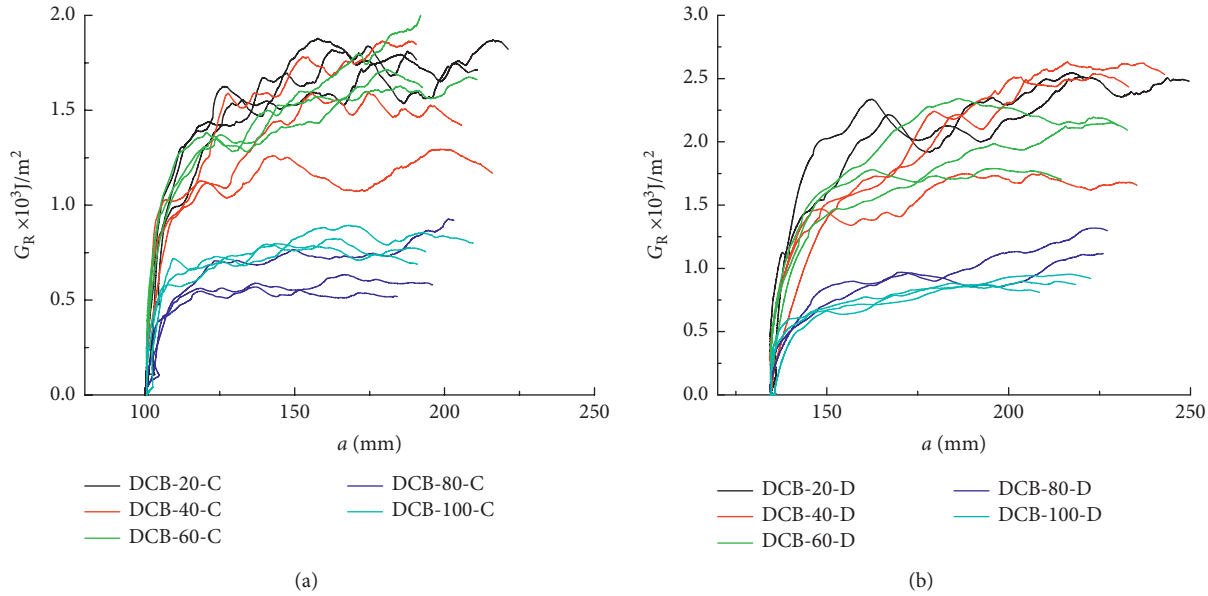

Figure 11: R-curves of DCB specimens with different widths in the same initial crack lengths. (a) Initial crack length $a_0 = 100$ mm. (b) Initial crack length $a_0 = 134$ mm.

Table 3: The average fracture toughness for partial test samples ($H = 50$ mm).

Specimens	a_0 (mm)	B (mm)	L (mm)	P (N)	G_R (J/m^2)
DCB-C	100	20	350	839	1740
		40		1535	1505
		60		2364	1550
		80		2149	630
		100		2952	820
DCB-D	134	20	350	745	2600
		40		1332	2570
		60		2081	1960
		80		2009	950
		100		2233	870

5. Conclusion

This paper has investigated an experimental procedure to obtain the energy release rate (ERR) using DCB tests for parallel strand bamboo (PSB) composites. The effects of specimen width and initial crack length on large-scale fiber bridging in Mode I fracture of unidirectional PSB composites were investigated. The R-curve measurements, for the range of the analyzed widths ($B = 20$, 40, 60, 80, and 100 mm) and initial crack lengths ($a_0 = 34$, 67, 100, and 134 mm), show that the energy release rate is influenced by both the width and initial crack length of specimens, in that the ERR at the plateau level decreased with an increasing width and initial crack length. Consequently, the DCB tests imply that the R-curve obtained in the present study is not a material property because it depends on the specimen geometry. However, the ERR at the plateau level is decreased to similar values as the width increases up to 80 mm and 100 mm. It may be concluded that the energy release rate would verge to a stable value with the width increasing up to more than a specific value, which can be clarified in the future DCB tests for PSB composites.

Nomenclature

B: Specimen width
C: Specimen compliance
a: Crack length
P: Applied load
G: Energy release rate
E: Young's modulus
h: Height of the cantilever portion, $H/2$
H: Specimen thickness
δ: Loading-line displacement
Δa: Crack extension
E_L: Elastic modulus in longitudinal direction
G_{LT}: Shear modulus in LT plane
I: Inertia moment of cross section
A: Area of cross section
λ: Calibration parameter to eliminate errors from experiments
$\overline{C}_0$: Theoretical compliance corresponding to initial crack length
C_0: Test compliance corresponding to the initial crack length
a_0: Initial crack length
v: Poisson's ratio
L: Specimen length.

Data Availability

The data of the DCB test for PSB composites used to support the findings of this study are available from the corresponding author upon request.

Conflicts of Interest

The authors declare that they have no conflicts of interest.

Acknowledgments

The research was supported by the National Natural Science Foundation of China (no. 51778299) and the Priority Academic Program Development of Jiangsu Higher Education Institutions.

References

[1] D. Huang, Y. Bian, A. Zhou, and B. Sheng, "Experimental study on stress-strain relationships and failure mechanisms of parallel strand bamboo made from phyllostachys," *Construction and Building Materials*, vol. 77, pp. 130–138, 2015.

[2] D. S. Huang, A. P. Zhou, H. T. Li, Y. Su, and G. Chen, "Experimental study on the tensile properties of bamboo related to its distribution of vascular bundles," *Key Engineering Materials*, vol. 517, pp. 112–117, 2012.

[3] D. Huang, A. Zhou, and Y. Bian, "Experimental and analytical study on the nonlinear bending of parallel strand bamboo beams," *Construction and Building Materials*, vol. 44, pp. 585–592, 2013.

[4] D. Huang, Y. Bian, D. Huang, A. Zhou, and B. Sheng, "An ultimate-state-based-model for inelastic analysis of intermediate slenderness PSB columns under eccentrically compressive load," *Construction and Building Materials*, vol. 94, pp. 306–314, 2015.

[5] M. F. Kanninen, "An augmented double cantilever beam model for studying crack propagation and arrest," *International Journal of Fracture*, vol. 9, pp. 83–92, 1973.

[6] R. Olsson, "A simplified improved beam analysis of the DCB specimen," *Composites Science and Technology*, vol. 43, no. 4, pp. 329–338, 1992.

[7] F. Ozdil and L. A. Carlsson, "Beam analysis of angle-ply laminate DCB specimens," *Composites Science & Technology*, vol. 59, no. 2, pp. 305–315, 1999.

[8] American Society for Test Materials (ASTM), *ASTM D5528-13, Standard Test Method for Mode I Interlaminar Fracture Toughness of Unidirectional Fiber-Reinforced Polymer Matrix Composite*, ASTM, West Conshohocken, PA, USA, 2013.

[9] H. Yoshihara and T. Kawamura, "Mode I fracture toughness estimation of wood by DCB test," *Composites Part A: Applied Science and Manufacturing*, vol. 37, no. 11, pp. 2105–2113, 2006.

[10] M. F. S. F. de Moura, J. J. L. Morais, and N. Dourado, "A new data reduction scheme for mode I wood fracture characterization using the double cantilever beam test," *Engineering Fracture Mechanics*, vol. 75, no. 13, pp. 3852–3865, 2008.

[11] J. De Gracia, A. Boyano, A. Arrese, and F. Mujika, "A new approach for determining the R-curve in DCB tests without optical measurements," *Engineering Fracture Mechanics*, vol. 135, pp. 274–285, 2015.

[12] American Society for Test Materials (ASTM), *ASTM D6671M-19, Standard Test Method for Mixed Mode I-Mode II Interlaminar Fracture Toughness of Unidirectional Fiber Reinforced Polymer Matrix Composites*, ASTM, West Conshohocken, PA, USA, 2019.

[13] International Organization for Standardization (ISO), *ISO 15024-2001, Fiber-reinforced Composite - Determination of Mode I Interlaminar Fracture Toughness, GIc, for Unidirectional Reinforced Materials*, ISO, Geneva, Switzerland, 2001.

[14] W. Xu and Z. Z. Guo, "A simple method for determining the mode I interlaminar fracture toughness of composite without measuring the growing crack length," *Engineering Fracture Mechanics*, vol. 191, pp. 476–485, 2018.

[15] D. Huang, B. Sheng, Y. Shen, and Y.-H. Chui, "An analytical solution for double cantilever beam based on elastic-plastic bilinear cohesive law: analysis for mode I fracture of fibrous composites," *Engineering Fracture Mechanics*, vol. 193, pp. 66–76, 2018.

[16] S. Hofmann, "Mode I delamination onset in carbon fibre reinforced SiC: double cantilever beam testing and cohesive zone modelling," *Engineering Fracture Mechanics*, vol. 182, pp. 506–520, 2017.

[17] E. Farmand-Ashtiani, J. Cugnoni, and J. Botsis, "Specimen thickness dependence of large scale fiber bridging in mode I interlaminar fracture of carbon epoxy composite," *International Journal of Solids and Structures*, vol. 55, pp. 58–65, 2015.

[18] A. Jyoti, R. F. Gibson, and G. M. Newaz, "Experimental studies of Mode I energy release rate in adhesively bonded width tapered composite DCB specimens," *Composites Science and Technology*, vol. 65, no. 1, pp. 9–18, 2005.

[19] N. A. Plan, S. Morel, and M. Chaplain, "Mixed-mode fracture in a quasi-brittle material: R-curve and fracture criterion—application to wood," *Engineering Fracture Mechanics*, vol. 156, pp. 96–113, 2016.

[20] S. Bennati and P. S. Valvo, "An experimental compliance calibration strategy for mixed-mode bending tests," *Procedia Materials Science*, vol. 3, pp. 1988–1993, 2014.

[21] S. Hashemi, A. J. Kinloch, and J. G. Williams, "Corrections needed in double-cantilever beam tests for assessing the interlaminar failure of fibrous-composites," *Journal of Material Science Letters*, vol. 8, no. 2, pp. 125–129, 1989.

[22] B. F. Sørensen and T. K. Jacobsen, "Large scale bridging in composites: R-curve and bridging laws," *Composites Part A*, vol. 29, no. 11, pp. 1443–1451, 1998.

[23] B. F. Sørensen, E. K. Gamstedt, R. C. Østergaard, and S. Goutianous, "Micromechanical model of cross-over fibre bridging-prediction of mixed mode bridging laws," *Mechanics of Materials*, vol. 40, no. 4-5, pp. 220–234, 2008.

[24] K. R. Pradeep, B. N. Rao, S. M. Srinivasan, and K. Balasubramaniam, "Interface fracture assessment on honeycomb sandwich composite DCB specimens," *Engineering Fracture Mechanics*, vol. 93, pp. 108–118, 2012.

[25] U. Stigh, "Damage and crack growth analysis of the double cantilever beam specimen," *International Journal of Fracture*, vol. 37, no. 1, pp. R13–R18, 1988.

[26] J. G. Williams, "End corrects for orthotropic DCB specimens," *Composite Science and Technology*, vol. 35, no. 4, pp. 367–376, 1989.

[27] L. P. Canal, M. Alfano, and J. Botsis, "A multi-scale based cohesive zone model for the analysis of thickness scaling effect in fiber bridging," *Composites Science and Technology*, vol. 139, pp. 90–98, 2017.

[28] B. D. Manshadi, E. Farmand-Ashtiani, J. Botsis, and A. P. Vassilopoulos, "An iterative analytical/experimental study of bridging in delamination of the double cantilever beam specimen," *Composites Part A: Applied Science and Manufacturing*, vol. 61, pp. 43–50, 2014.

[29] H. Danielsson and P. J. Gustafsson, "A three dimensional plasticity model for perpendicular to grain cohesive fracture in wood," *Engineering Fracture Mechanics*, vol. 98, pp. 137–152, 2013.

[30] A. B. de Morais, "A new fibre bridging based analysis of the double cantilever beam (DCB) test," *Composites: Part A*, vol. 42, no. 10, pp. 1361–1368, 2011.

[31] S. Morel, C. Lespine, J. L. Coureau, J. Planas, and N. Dourado, "Bilinear softening parameters and equivalent LEFM R-curve

in quasibrittle failure," *International Journal of Solids and Structures*, vol. 47, no. 6, pp. 837–850, 2010.

[32] J.-L. Coureau, S. Morel, and N. Dourado, "Cohesive zone model and quasibrittle failure of wood: a new light on the adapted specimen geometries for fracture tests," *Engineering Fracture Mechanics*, vol. 109, pp. 328–340, 2013.

[33] Z. P. Bazant and M. T. Kazemi, "Size effect in fracture of ceramics and its use to determine fracture energy and effective process zone length," *Journal of the American Ceramic Society*, vol. 73, no. 7, pp. 1841–1851, 1990.

[34] F. A. M. Pereira, M. F. S. F. de Moura, D. Dourado, J. J. L. Morais, J. Xavier, and M. I. R. Dias, "Direct and inverse method to the determination of cohesive law of bovine cortical bone using the DCB test," *International Journal of Solids and Structures*, vol. 128, pp. 210–220, 2017.

[35] American Society for Test Materials (ASTM), *ASTM D143-14, Standard Test Methods for Small Clear Specimens of Timber*, ASTM, West Conshohocken, PA, USA, 2014.

[36] H. D. Bui, *Fracture Mechanics*, Springer, Berlin, Germany, 2006.